All-sky assimilation of SSMI/S humidity sounding channels over land

Fabrizio Baordo, Alan Geer and Stephen English

ECMWF, Shinfield Park, Reading
RG2 9AX, United Kingdom
F.Baordo@ecmwf.int

ABSTRACT

The all-sky assimilation of microwave radiances over ocean is a well established framework within the ECMWF operational system. Recently, the all-sky package over ocean has been updated in order to improve the simulated microwave radiances. Better scattering radiative transfer calculations, based on discrete dipole simulations to represent optical properties of snow hydrometeors, have brought the possibility of assimilating higher microwave frequencies such as SSMI/S 183 GHz channels. This upgrade has been found beneficial for winds and humidity analysis and forecasts. Considering the importance of such improvements, investigations have been carried out in order to have an equivalent all-sky framework over land to assimilate SSMI/S humidity sounding channels. This paper not only describes the necessary changes to develop the over land framework, but also scientifically evaluates the impact of the assimilation on analysis and forecast. The findings of this study show that the all-sky assimilation over land is reliable and it brings positive improvements into the system which can be seen in terms of both forecast scores and fits to conventional and other satellite observations.

1 Introduction

The possibility of extending the all-sky framework over ocean (Geer and Bauer, 2010, 2011, Bauer et al., 2010) to land surfaces was initially investigated by Baordo et al. (2012). The results of that investigation were mainly two: a) it is feasible to consider a land surface emissivity retrieval from satellite observations in all-sky conditions; b) deficiencies in radiative transfer calculations, mainly due to the use of Mie sphere to represent frozen hydrometeors, generally restrict developments of assimilating higher microwave frequencies such as SSMI/S humidity sounding channels.

Recently, in order to obtain more realistic simulated brightness temperature, Geer and Baordo (2013) investigated the choice of modelling scattering radiative transfer using the discrete dipole approximation (DDA) to represent the optical properties of snow hydrometeors. This study found that the use of DDA sector snowflakes (Liu, 2008) to represent the optical properties of snow hydrometeors, improves the global simulation of microwave radiances compare to the inappropriate assumption of Mie spheres. The modified all-sky package over ocean will be introduced in the IFS cycle 40r1 and the benefits obtained are documented by Geer (2013). In the same way, the advantages of better radiative transfer calculations have been additionally explored in order to build an equivalent framework to also assimilate SSMI/S humidity sounding channels over land in all-sky conditions.

This paper, firstly, describes the methodology adopted to develop the over land framework and, secondly, through forecast scores and fits to conventional and other satellite observations, evaluates the impact of the assimilation on the ECMWF system. Additional details of the all-sky assimilation over land of SSMI/S humidity sounding channels are provided by Baordo et al. (2013).

2 All-sky assimilation general overview

The observation operator designed for assimilating microwave radiances in all-sky conditions is RTTOV-SCATT (Bauer et al., 2006). This uses the delta-Eddington approximation (Joseph et al., 1976) to solve the radiative transfer equation including scattering. Two liquid and two frozen hydrometeors types are provided by IFS to RTTOV-SCATT: cloud water, rain, cloud ice and snow. The optical properties of each particle are taken from look-up tables: cloud water, rain and cloud ice are considered as a sphere and modelled using Mie theory, while snow hydrometeors are represented by DDA sector snowflakes (Liu 2008). Land surface emissivity is retrieved from satellite observations (Baordo et al., 2012) and assessed by emissivity estimates from TELSEM (Tool to Estimate Land Surface Emissivities at Microwave frequencies, Aires et al., 2010), a package available within RTTOV, containing pre-calculated monthly mean emissivity climatology derived from ten-year SSM/I observations. Ocean surface emissivity is computed using version 5 of FASTEM (Liu et al., 2011). The simulated brightness temperature is computed considering the contribution from two independent sub-columns: a clear column, taking into account only gaseous absorption, and a cloudy column additionally taking into account cloud, precipitation and scattering. The two sub-columns are weighted according to the effective cloud fraction (Geer et al., 2009), depending not only on the hydrometeor amount (cloud liquid, cloud ice, rain and snow) but also on the convective and large-scale precipitation fractions at each layer of the atmosphere. Complete details of the all-sky assimilation are given by Geer and Bauer (2010, 2011) and Bauer et al. (2010).

3 Methodology

In order to develop the all-sky framework over land and achieve the assimilation of SSMI/S humidity sounding observations, technical and scientific changes within the ECMWF system have been required. The all-sky package over land is basically characterised by 3 main developments. Their important features are summarised below.

1. **Discrete dipole approximation (DDA) to represent the optical properties of snow hydrometeors.**
   Deficiencies in radiative transfer calculations, mainly due to the use of Mie sphere to represent frozen hydrometeors, have restricted developments of all-sky assimilation wherever scattering effects are dominant (for instance over land surfaces or in temperature and humidity sounding channels). Recently, in order to obtain more realistic simulated brightness temperatures, Geer and Baordo (2013) investigated the choice of which DDA particle shape is optimal to represent the optical properties of snow hydrometeors in the all-sky radiative transfer calculations. Replacing Mie sphere approximation with more realistic DDA sector snowflakes largely improves the global simulation of microwave radiances. However, there is a difference to take into account between ocean and land surfaces. Over ocean, all-sky brightness temperatures are computed and weighted according the effective cloud fraction (‘Cav’ approach). Over land, instead, the best agreement between simulated and observed radiances is obtained when the effective cloud fraction is replaced by the largest cloud fraction in the model profile (‘Cmax’ approach). This result is summarised in Figure 1 for SSMI/S channel 9 (183$\pm$7 GHz). This outcome is questionable considering the that the ‘Cav’ approach is thought to be more physically realistic. However, one explanation might be in the forecast model bias between ocean and land: the model seems to produce less deep convection over land than over ocean in contrast to observations which indicate more convective areas over land. This might be the reason for the beneficial impact of the ‘Cmax’ approach over land which helps to increase the amount of scattering producing colder simulated brightness temperatures.

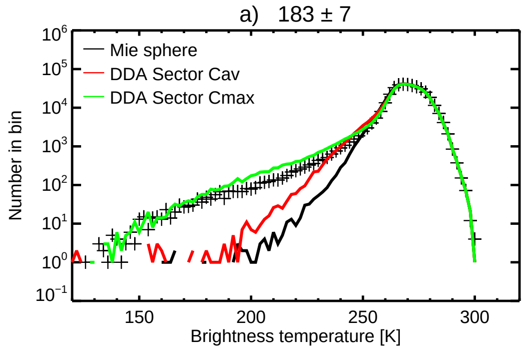

Figure 1: Histogram of observed (black cross) and simulated brightness temperatures at 183±7 GHz using Mie sphere approximation (balck line) and DDA sector snowflakes with 'Cav' (red line) or 'Cmax' (green line) approach. Sample of SSMI/S observations is over land between 60°S and 60°N. Bin size is 2.0 K.

2. **Surface emissivity estimates.**
Land surface emissivity estimates can be obtained using satellite observations, a method commonly adopted in literature (i.e. Prigent et al., 2005). In the all-sky approach, the implementation of the emissivity retrieval from satellite data was coded within the scattering radiative transfer code so that the emissivity estimate takes into account cloud and precipitation (Baordo et al., 2012). Even though cloud is simulated in the observation operator in the all-sky approach, the model forecast will not always put it in the right place. Cloud contamination is still a problem where model does not forecast cloud but it is there in the observations. Table 1, comparing emissivity estimates obtained from SSMI/S window channels to those provided by TELSEM, encapsulates the nature of this problem. SSMI/S observations are for a geographical location not affected by critical orography or surface temperature conditions: orography is less than 500 meters and surface temperature is 295 K. Moving from 19 to 91 GHz, the higher is the microwave frequency, the larger is the depression in the radiances: channels at 37 GHz and 91 GHz are, respectively, 15-20 K and about 60 K colder than those at 19 GHz. Cloud contamination is not an issue for low frequencies and, hence, 19 GHz channels bring realistic emissivity estimates, similar to those provided by TELSEM. Emissivity retrievals at higher frequencies (37 GHz) begin to be affected by cloud contamination and the resultant emissivity estimations are slightly lower than TELSEM, but they still might be considered reasonable (for instance, cloud and precipitation might produce changes in surface conditions such as soil moisture or temperature). Channels at 91 GHz, instead, are those mostly affected by cloud contamination and as a consequence the resultant emissivity retrievals are completely unrealistic. In the all-sky framework, emissivities are retrieved from satellite observations at window channels and then these estimates are assigned to higher frequencies according to the right polarisation in order to perform radiative transfer calculations. To take into account cloud contamination issues which might cause unrealistic emissivity estimates, emissivities from TELSEM are used to guide the choice of keeping or rejecting the retrieval.

3. **Observation error modelling.**
The all-sky assimilation over ocean predicts the total error of FG departures as a function of the symmetric cloud amount given by the average of observed and simulated polarisation difference at 37 GHz. To estimate the total error of FG departure over land we followed an equivalent approach, but the scattering index (SI) given by frequencies difference at SSMI/S channel 18 and channel 8 (respectively, 91 GHZ and 150 GHZ, horizontal polarisations) has been chosen as the symmetric predictor. Figure 2 shows how the standard deviation of SSMI/S channel 9 (183±7 GHz) FG departures have been modelled in order to have an observation error formulation. This

SSMI/S channel	19h	19v	37h	37v	91h	91v
Brightness Temperature [K]	285.32	283.42	268.81	269.18	222.67	225.66
Emissivity retrieved	0.947	0.944	0.881	0.884	0.284	0.357
Emissivity from TELSEM	0.966	0.971	0.954	0.959	0.951	0.956

Table 1: Cloud contamination impact on emissivity retrievals obtained using SSMI/S observations over land. Set of observations are for 1^{st} June 2012, over the North-East of China near the Russian border.

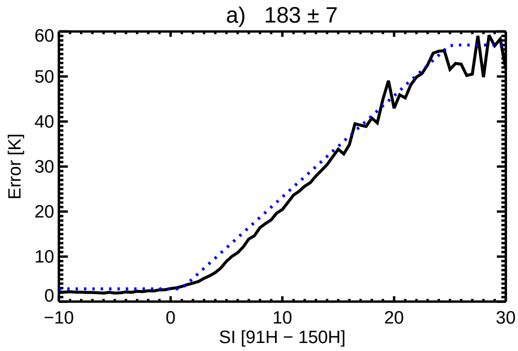

Figure 2: Error model for SSMI/S channel 9 (183$\pm$7 GHz), showing how the standard deviations of FG departures binned as a function of symmetric scatting index (black solid line) are modelled by a linear fit (blue dashed line). Statistics are for those observations over land between 60°S and 60°N. Bin size is 0.5 K.

approach identifies two main areas: a region where the error can be estimated as a constant value and a second region, instead, where the error can be approximated by a linear fit. The first region can be interpreted as the clear-sky area where observations are unaffected by scattering and presumably free of cloud and precipitation. In this area, the total error for SSMI/S humidity sounding channels is constant and equal to 3 K. This error is comparable to the observation error used for the equivalent MHS channels which are assimilated in clear-sky conditions and have a 2 K error. The second region represents the area where there may be cloud or precipitation in model or observation and the influence of scattering increases as well as the standard deviations of FG departures. It is also worth mentioning that observations in Figure 2 have been selected considering the same surface screening criteria currently used operationally at ECMWF to assimilate MHS humidity sounding channels over land in clear-sky conditions. Observations are rejected according to surface temperature and orography thresholds to avoid snow-covered surfaces and scenes where the surface might be the dominant part of the radiative transfer.

4 All-sky assimilation impact

Control and assimilation experiments were set up in order to evaluate the impact on analyses and forecasts of assimilating SSMI/S 183 GHz channels over land in the all-sky approach. Experiments, covering a 3 month period (June to August 2012), were run at T511 horizontal resolution and 137 vertical levels in a 4D-Var 12 hour assimilation window. The control experiment also includes the changes of the all-sky package over ocean (Geer 2013). In this way, outcomes from the all-sky assimilation experiment over land can be evaluated as the result produced on top of the all-sky over ocean upgrade which will be supplied for cycle 40r1. Details of control and experiment can be summarised as follows:

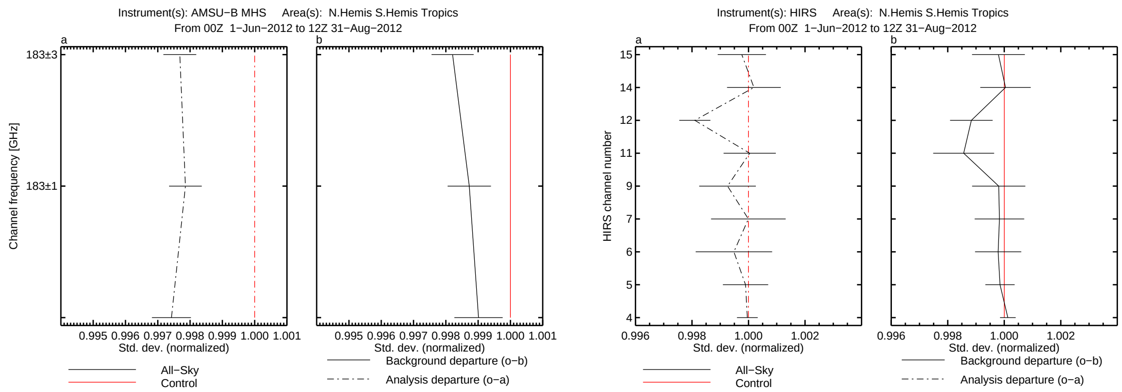

Figure 3: Normalised change in standard deviation of analysis departures (a) and FG forecast departures (b) for global MHS (from NOAA-18, NOAA-19 and Metop-A), left column, and HIRS observations (from NOAA-19 and Metop-A), right column. Standard deviations are normalised by those of the control experiment. Error bars indicate the 95% confidence level. Statistics are for a 3 month period (June to August 2012).

- Control: 38r2 observing system + all-sky over ocean package + SSMI/S observations over land introduced passively into the system.
- All-sky assimilation experiment: as Control, but SSMI/S 183 GHz channels actively assimilated over land using the all-sky developments: radiative transfer calculations upgrade (DDA sector and 'Cmax' approach) + surface emissivity retrieval + observation error formulation.

To investigate the impact of the all-sky assimilation we can rely on fits to other assimilated observations. This approach gives us an estimate of the effectiveness of the new observations assimilated into the system. Reduction in standard deviations of FG forecast departures is a sign that the system, assimilating new observations, is moving towards the right direction and, as a consequence, the resultant atmospheric background, which represents a short forecast from the previous analysis, is improving. Water vapour sensitive channels from MHS (183 GHz channels) and HIRS (channel 11 and 12) are actively assimilated into the system and, as a consequence, these instruments can be used to evaluate the impact of the assimilation of SSMI/S humidity sounding observations. Fits to MHS (from NOAA-18, NOAA-19 and Metop-A) and HIRS (from NOAA-19 and Metop-A) observations are analysed through Figure 3. The overall result is generally positive considering that the all-sky assimilation globally brings statistically significant reductions in standard deviations of FG forecast departures. Fits to conventional observations are also important to evaluate. Figure 4 shows analysis fits to wind conventional observations (combining TEMP-U and TEMP-V) in the Southern and Northern hemisphere. Results indicate that standard deviation of FG forecast departures are generally reduced compared to the control: the all-sky approach brings statistically significant reductions of about 0.4% at 700 hPa in the Southern hemisphere and about 0.2% at 500 hPa and 300 hPa in the Northern hemisphere. The impact of water vapour sounding channels on wind fields might be explained by the 4D-Var tracer effect. The feature-tracing of water vapour, cloud and precipitation structures likely leads to a better adjustments of the wind fields and, as a result, also a small number of assimilated cloud affected observations might play an important role in the wind analysis and forecast.

Additional verification of the link between the all-sky assimilation and the 4D-Var tracing effect can be evaluated looking at the normalised change in the RMS forecast error of vector wind at 200 hPa, 500 hPa and 850 hPa for the Southern (-90° to -20°) and Northern (20° to 90°) hemisphere (Figure 5). The all-sky experiment is compared to the control ('Experiment minus Control') and negative values indicate reduce RMS forecast errors, hence an improvement respect to the control. Using the all-sky assimilation,

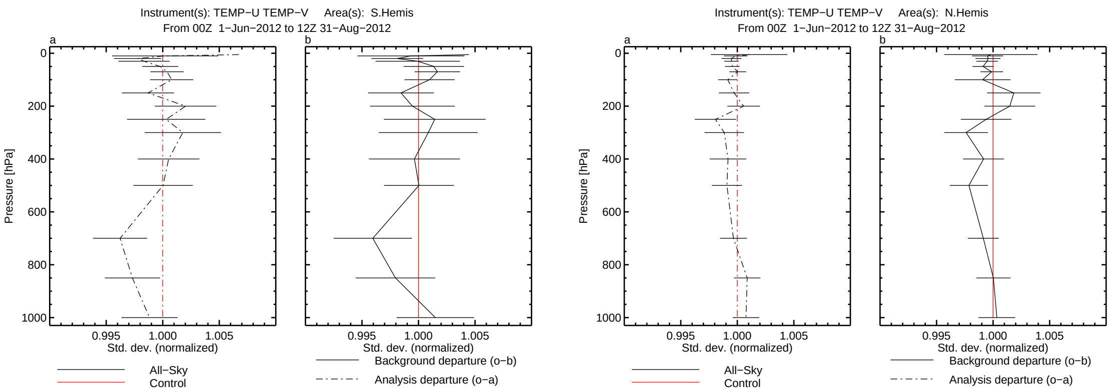

Figure 4: Normalised change in standard deviation of analysis departures (a) and FG forecast departures (b) for wind observations (TEMP-U and TEMP-V). Left column and right column show, respectively, fits for the Southern and the Northern hemisphere. Standard deviations are normalised by those of the control experiment. Error bars indicate the 95% confidence level. Statistics are for a 3 month period (June to August 2012).

RMS errors in vector wind are reduced from the lower to the upper part of the troposphere in both the Southern and Northern hemisphere. RMS errors appear to decrease at shorter ranges and increase, not significantly, at longer ranges (day 6, 7 and 8). Statistically significant reductions are observed in both the hemispheres: for instance, at 850 hPa in the Southern hemisphere, RMS error reduction of about 1% is observed at day 3 and about 0.5% at day 2 and 4, while in the Northern hemisphere, day 3, 4 and 5 are characterised by a decrease of about 0.5%.

5 Conclusions

The overall outcome of this study not only demonstrates the feasibility of the all-sky package over land, but also shows the beneficial impact on the system of assimilating humidity sounding channels in all-sky conditions. The latter has been evaluated in terms of both fits to other satellite observations and forecasts scores. The all-sky approach is effective at improving wind fields, confirming similar findings that showed up when the SSMI/S 183 GHz channels were initially assimilated in the all-sky approach over ocean. The 4D-Var tracer effect is the probable cause of such improvements. While the system is already fed with many other microwave humidity sounding observations both over ocean and land, cloud and precipitation structures might lead to a better adjustments of the wind fields and, as a result, a small number of assimilated cloud affected observations might play an important rule in the wind analysis and forecast. A new investigation has already started within the ECMWF system in order to validate the all-sky package over land presented in this paper. Firstly, the all-sky assimilation of SSMI/S humidity sounding channels will be again evaluated within the ECMWF 39r1 cycle, and, secondly, the all-sky package over land will be also applied to MHS observations in order to investigate the possibility of assimilate MHS data in all-sky conditions over both ocean and land. The all-sky package over land will be likely considered for the future operational IFS cycle 40r2.

Acknowledgements

Fabrizio Baordo is funded through the EUMETSAT fellowship programme.

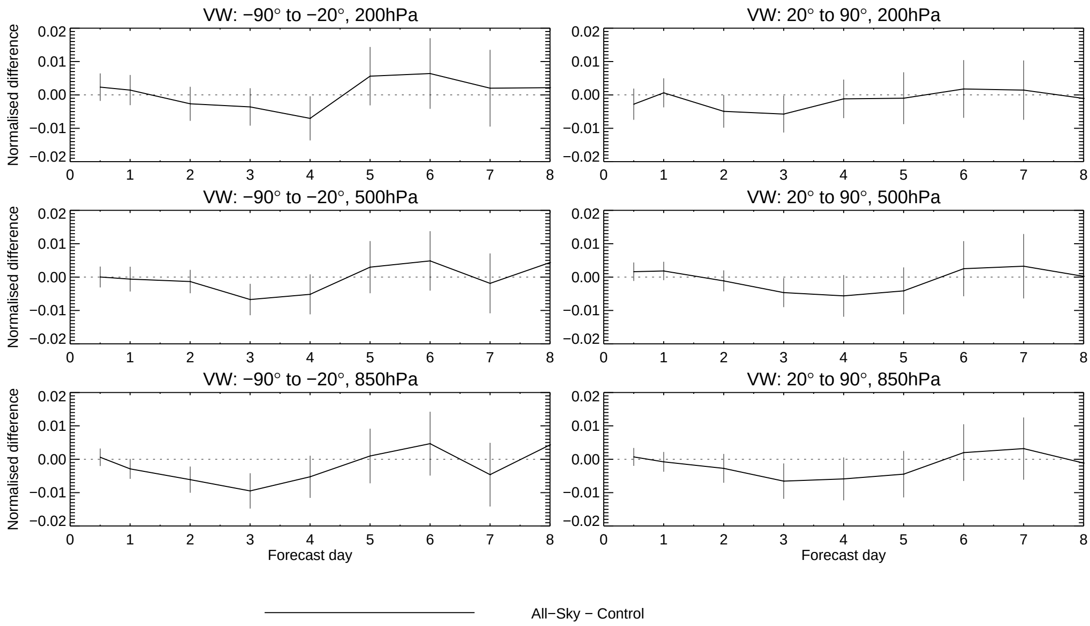

Figure 5: Normalised change in RMS forecast error in vector wind at 200 hPa (top row), 500 hPa (middle row) and 850 hPa (bottom row) for the Southern (-90° to -20°) and Northern (20° to 90°) hemisphere. Verification is against own analysis. Scores are based on a 3 month period (June to August 2012). Error bars indicate the 95% confidence level.

References

Aires F., Prigent C., Bernado F., Jimnez C., Saunders R. and Brunel P., 2010. A tool to estimate Land Surface-Emissivities at Microwaves frequencies (TELSEM) for use in numerical weather prediction. Q. J. R. Meteorol. Soc. 137, 690–699.

Baordo F., Geer A. J. and English S., 2012. SSMI/S radiances over land in the all-sky framework: one year report. EUMETSAT/ECMWF Fellowship Programme Research Report No. 27, available from http://www.ecmwf.int.

Baordo F., Geer A. J. and English S., 2013. All-sky assimilation of SSMI/S humidity sounding channles over land: second year report. EUMETSAT/ECMWF Fellowship Programme Research Report No. 30, available from http://www.ecmwf.int.

Bauer P., Moreau E., Chevallier F. and OKeeffe U., 2006. Multiple-scattering microwave radiative transfer for data assimilation applications. Q. J. R. Meteorol. Soc. 132, 1259–1281.

Bauer P., Geer A. J., Lopez P. and Salmond D., 2010. Direct 4D-Var assimilation of all-sky radiances. Part I: Implementation. Q. J. R. Meteorol. Soc. 136, 1868–1885.

Geer A. J., Bauer P. and ODell C.W., 2009. A revised cloud overlap scheme for fast microwave radiative transfer in rain and cloud. J. Applied Meteorology, 48, 2257–2270.

Geer A. J. and Bauer P., 2010. Enhanced use of all-sky microwave observations sensitive to water vapour, cloud and precipitation. Published simultaneously as ECMWF Technical Memoranda 620 and ECMWF/EUMETSAT fellowship reports 20.

Geer A. J., Bauer P. and Lopez P., 2010. Direct 4D-Var assimilation of all-sky radiances: Part II. Assessment. Q. J. R. Meteorol. Soc. 136, 1886–1905.

Geer A. J. and Bauer P., 2011. Observation errors in all-sky data assimilation. Q.J.R. Meteorol. Soc. 137: 2024–2037.

Geer A. J., Bauer P. and English S., 2012. Assimilating AMSU-A temperature sounding channels in the presence of cloud and precipitation. ECMWF, available from http://www.ecmwf.int.

Geer A. J. and Baordo F., 2013. Improved scattering radiative transfer for frozen hydrometeors at microwave frequencies. To be submitted.

Geer A. J., 2013. All-sky assimilation: better snow-scattering radiative transfer and addition of SSMI/S humidity sounding channels. To be submitted.

Joseph J., Wiscombe W. J. and Weinman J. A., 1976. The delta-Eddington approximation for radiative flux transfer. J. Atmos. Sci. 33, 2452–2459.

Liu G., 2008. A database of microwave single-scattering properties for non spherical ice particles. Bull. Am. Met. Soc. 111, 1563–1570.

Liu Q., Weng F. and English S., 2011. An Improved Fast Microwave Water Emissivity Model. IEEE Trans. on Geoscience and Remote Sensing, 49, 4, 1238–1250.

Prigent C., Chevallier F., Karbou F., Bauer P. and Kelly G., 2005. AMSU-A surface emissivities for numerical weather prediction assimilation schemes. J. Applied Meteorology, 44, 416–426.